International Journal of Mathematics Trends and Technology
ISSN: 2231 – 5373 /doi:10.14445/22315373/IJMTT-V67I5P515
Volume 67 Issue 5, 126-149, May, 2021

Onset of Transition to Non-Newtonian MHD Chemically Reacting Couette Copper Nanofluid Flow in a Radiative Porous Medium

[1]Ngiangia Alalibo, [2]Orukari Mercy., [3]Amadi Okeychukwu., [1]Nwabuzor Peter

[1] *Department of Physics, University of Port Harcourt, P M B 5323 Choba, Port Harcourt, Nigeria*
[2] *Department of Mathematics and Computer Science, Niger Delta University, Wilberforce Island, Nigeria*
[3] *Department of Mathematics, Ignatius Ajuru University of Education, Rumuolumeni, Nigeria*

Abstract
Thermo-physical data of copper nanoparticles in water based nanofluid in cylindrical Couette flow regime was investigated. The governing momentum, energy and specie concentration equations were transformed into dimensionless form and a regular perturbation and approximation with Frobenius method were used and solutions obtained to determine the effect of some chosen material parameters in the presence and absence of Brownian motion. Analyses of the results show that an early onset of transition from Newtonian fluid to non-Newtonian fluid was observed when the Reynolds number is still within Newtonian fluid domain. Effect of the material parameters considered on the skin friction, rate of heat and mass transfer coefficients were discussed as well as calculation of mass flux, mean temperature and mean specie concentration of the copper nanofluid.

Keywords: *Brownian motion, Couette flow, Copper nanoparticles, Magnetohydrodynamics (MHD), Porous Medium.*

I. INTRODUCTION
Couette, studied the flow of fluid with its motion brought about by the relative movement of two concentric cylinders of varying radii. It is a flow of viscous incompressible fluid between two infinite parallel plates separated by a distance (d). A typical example of Couette flow is the earth and atmosphere with its constituents between them. The study of fluid flows through porous plates, surfaces or media cannot be overemphasized. Many natural and physical processes, such as the movement of xylem and phloem cells in plants, perspiration in animals and diffusion through permeable membrane involve the flow of fluid. The search for fluids with improved thermal conductivity and viscosity led Choi [1], to call a mixture nanofluid. The mixture is said to be a colloidal suspension composed of a base fluid and nanoparticles with sizes in the range 1nm – 100nm. Materials in nano-scale show surprising physical, chemical, biological, mechanical and electrical properties compared to some materials at higher scale. The enhanced or improved heat transfer properties of nanofluids make its applications in cooling technologies, nuclear reactors and transport desirable. Others are electronics and biomedicine [2]. The transport phenomena around cylindrical objects which Couette flow is key are subjects of great value in practical and theoretical studies with their attendant industrial importance. Thermal exposure of foods and cooling of electronics are few of the areas it is applied. The importance of fluid as a heat transfer medium largely depends on its heat transfer efficiency that can be studied from the thermo-physical properties of the fluid. One cardinal property of nanofluids is that, a sizeable quantity of nanoparticles is what is required to add to a base fluid and an exceptional heat enhancement property several times more expected theoretically. These improved properties of nanofluid over and above conventional base fluids are found to improve efficiency and reduce cost. Take to be a bridge between cutting edge nanotechnology and traditional thermal science, nanofluids have established itself as modern heat transfer media with far improved heat transfer potentials. Theoretical (Singh [3]) and experimental (Bearman [4], Angrilli et al [5], Taniguchi and Miyakoshi [6]), studies in flow and heat transport of circular cylinder were carried out because of its application in process industries. Some studies of nanofluids flow in different geometries are abounded. The transient free convection flow of nanoparticles between two long parallel plates was investigated by Narahari et al [7] and useful deductions on the wall temperature and wall heat flux were made. Azhar et al [8], opined that heat transfer fluid flows enhancement is more pronounced in fractional nanofluids than in ordinary nanofluids in the study of free convection flow of some water based fractional nanofluids over a moving infinite vertical plate. Santra et al [9], carried out a study on heat transfer due to copper oxide in water based nanofluid between two parallel plates maintained at equal temperatures for Reynolds number with laminar flow regime and nanoparticles volume fractions. Sandip et al [10], stated that vortex formation exhibits symmetric wave characteristics in the study of symmetric vorticity distribution on circular cylinders in cross flow for different volume fractions of water based nanofluids. Ahmed et al [11], reported that the Nusselt number

increases in the study of a squeezed nanofluid flow between two parallel plates. Study of models of both single phase and multi phase nanofluid and their solutions were carried out by Turkyilmazoglu [12] and the results showed that the Nusselt number is enhanced as the diffusion parameter in the multi phase model increases. Laplace transform technique was employed by Loganathan et al [13] to analyze the effects of heat generation and nanoparticle volume concentration on an unsteady free convective flow of a nanofluid past an impulsively started infinite vertical plate. Hajizadeh et al [14], investigated the free convection flow of nanofluids between two vertical plates with damped thermal flux and comparison between the fluids with thermal memory and the ordinary fluid is made. Brownian motion is one of the concepts for the thermal conductivity enhancement of nanofluids. Its principle helps in manufacturing communication engineering silicon and germanium oxide optical fibers. A nanoflow past a horizontal circular cylinder considering the twin effect of Brownian motion and thermophoresis was investigated by Reddy et al [15] and their deductions supported the enhancement of thermal conductivity by Brownian motion. The same effect of thermophoresis and Brownian motion was considered by Sacharitha et al [16] on slip nanoflow past symmetric channel while kandasamy et al [17] and Ambuchezhian et al [18] studied the effect together with thermal stratification of a nanofluid. Some studies such as Xuan et al [19], Das et al [20], Kumar et al [21] and Bhattacharya et al [22], in their models proposed, were criticized that the Brownian motion is a weak factor in the determination of thermal conductivity enhancement. Magnetic fields exist everywhere in space, it implies that Magnetohydrodynamics (MHD) phenomena must occur wherever conducting fluids are available. For a particular liquid metal MHD, magnetic fields are used to levitate samples of liquid metal and to control their shape. The advent of studies of thermonuclear fusion reaction enhanced problems associated with the behaviour of a high temperature plasmas in a magnetic field. As a result of the wide application of magnetic field, Reddy et al [23], Sreenivasulu et al [24], Tamoror [25], Parida et al [26], Nayak et al [27], Abbas et al [28] and Souayeh et al [29] all tackled the effect of magnetic Hartmann number in the study of their different fluid flow regimes. Based on the aforementioned features and applications, our proposed study on MHD Couette flow of nanofluid in a radiative porous medium is to among other considerations, compare the presence and absence of Brownian motion on the temperature and velocity profiles of the Couette copper nanoparticles in water based fluid, determine the transition to non-Newtonian fluid flow using Reynolds number regime as well as the calculation of skin friction, rate of heat transfer coefficient and rate of mass transfer coefficient.

II. MODELING THE PHYSICAL PROBLEM

The flow of copper nanofluid within two infinite concentric cylindrical surfaces of inner and outer radii r' and $r*$ respectively, having distance of separation d. The inner cylinder is moving upward and downward while the outer cylinder is at rest. The governing partial differential equations in cylindrical form are given as

$$\frac{\partial \rho_{nf}}{\partial t'} + \frac{1}{r'}\frac{\partial}{\partial r'}\left(\rho_{nf} r v_r\right) = 0 \tag{1}$$

$$\frac{\partial v_r}{\partial t'} + v_r \frac{\partial v_r}{\partial r'} = \frac{\mu_{nf}}{\rho_{nf}}\left(\frac{\partial^2 v_r}{\partial r'^2} + \frac{1}{r'}\frac{\partial v_r}{\partial r'} - \frac{v_r}{r'^2}\right) + g\beta_{nf}\left(T - T_0\right) + g\beta'_{nf}\left(C' - C_0\right) - \frac{\upsilon}{\rho_{nf}\kappa} v_r - \frac{\sigma B_0^2 v_r}{\rho_{nf}} \tag{2}$$

$$\frac{\partial T}{\partial t'} + v_r \frac{\partial T}{\partial r'} = \frac{k_{nf}}{\left(\rho C_p\right)_{nf}}\left(\frac{1}{r'}\frac{\partial T}{\partial t'} + \frac{\partial^2 T}{\partial r'^2}\right) - \frac{1}{\left(\rho C_p\right)_{nf}}\frac{\partial q_r}{\partial r'} \tag{3}$$

$$\frac{\partial C'}{\partial t'} + v_r \frac{\partial C'}{\partial r'} = \frac{D}{\left(\rho C_p\right)_{nf}}\left(\frac{1}{r'}\frac{\partial C'}{\partial t'} + \frac{\partial^2 C'}{\partial r'^2}\right) - \frac{1}{\left(\rho C_p\right)_{nf}} k_r^2 C' \tag{4}$$

Subject to the Couette flow boundary conditions $v_r(0,t) = 0, v_r(d,t) = U$, $T(0,t) = 1, T(\infty,0) = 0$, $C'(0,t) = 1, C'(\infty,t) = 0$ (Ngiangia and Orukari [30])

where v_r is velocity of nanofluid, r' is radius of nanoparticles, t' is time, C' is nanofluid concentration, ρ_{nf} is density of nanofluid, μ_{nf} is viscosity of nanofluid, σ is electrical conductivity of base fluid, B is imposed magnetic induction, g is acceleration due to gravity, β_{nf} is thermal expansion due to temperature, β'_{nf} is thermal expansion due to concentration, T is temperature of nanofluid, T_0 is free stream temperature, C_0 is free stream concentration, k_{nf} is thermal conductivity of nanofluid, $\left(C_p\right)_{nf}$ is specific heat at constant pressure of nanofluid, q_r is radiation term, k_r^2 is chemical reaction term, D is chemical molecular diffusivity, d is distance between the plates and U is characteristic velocity

In order to consider the effect of radiation on an optically thick model in which the thermal layer becomes very thick or highly absorbing as described by Rosseland approximation, Cogley et al [31] as

$$\frac{\partial q_r}{\partial r'} = -\frac{4k_B}{3\alpha}\frac{\partial T^4}{\partial r'} \tag{5}$$

where k_B is the Stefan-Boltzmann constant and α is the absorption coefficient. If temperature difference within the flow of the nanofluid is sufficiently small, we can approximate T^4 using Taylor series expansion about T_∞ and neglect higher order terms, the expression results into

$$T^4 = 4T_\infty^3 T - 3T_\infty^4 \tag{6}$$

According to Hamilton and Crosser model [32], effective dynamic viscosity and effective thermal conductivity which are valid for both spherical and non spherical shapes nanoparticles are defined as

$$\frac{\mu_{nf}}{\mu_f} = \left(1 + a\phi + b\phi^2\right) \tag{7a}$$

and

$$\frac{k_{nf}}{k_f} = \frac{k_s + (n-1)k_f + (n-1)(k_s - k_f)\phi}{k_s + (n-1)k_f - (k_s - k_f)\phi} \tag{7b}$$

Following the model proposed by Koo and Kleinstrever ([33 and 34]) in determining the thermal conductivity enhancement, a modification proposed by Ngiangia and Nwabuzor [35] is given as

$$\frac{k_{nf}}{k_f} = \frac{k_s + (n-1)k_f + (n-1)(k_s - k_f)\phi}{k_s + (n-1)k_f - (k_s - k_f)\phi} + 5x10^4 \xi\phi\left(\rho C_p\right)_s \sqrt{\frac{k_B T}{\rho_s D_s}}\, f(T,\phi) \tag{7c}$$

The function $f(T,\phi)$ can vary continuously with particle volume fraction as $f(T,\phi) = (-6.04\phi + 0.4705)T + (1722.30\phi - 134.63)$.

The empirical shape factor is given by $n = 3\psi^{-1}$, ψ is the sphericity, ξ is related to particle motion, k_f and k_s are thermal conductivities of base fluid and solid nanoparticles respectively. According to the work of Tiwari and Das [36] and Asma et al [37], density of nanofluid (ρ_{nf}), thermal expansion due to temperature of nanofluid (β_{nf}), thermal expansion due to concentration of nanofluid (β'_{nf}), specific heat at constant pressure of nanofluid $\left(C_p\right)_{nf}$ are respectively

$$\rho_{nf} = (1-\phi)\rho_f + \phi\rho_s$$

$$\begin{aligned}\beta_{nf} &= (1-\phi)\beta_f + \phi\beta_s \\ \beta'_{nf} &= (1-\phi)\beta'_f + \phi\beta'_s \\ (C_p)_{nf} &= (1-\phi)(C_p)_f + \phi(C_p)_s\end{aligned} \tag{8}$$

where the nanoparticles volume fractions is given by $\phi = m\frac{\pi}{6}D_s$, m is the number of particles per unit volume and D_s is the average diameter of the particles, ρ_f and ρ_s are the densities of the base fluid and solid nanoparticles, β_f and β_s are the thermal expansion due to temperature of base fluid and solid nanoparticles, β'_f and β'_s are the thermal expansion due to concentration of base fluid and solid nanoparticles and $(C_p)_f$ and $(C_p)_s$ are the specific heat at constant pressure due to base fluid and solid nanoparticles.

Dimensional Analysis

Dimensional homogeneity of the governing nanofluid equations using the Buckinham-π – theorem is stated

$$u = \frac{v_r t'}{r'}, r = \frac{r'}{d}, t = \frac{t'}{u'r'}, \mathrm{Re}^{-1} = \frac{\mu_{nf}\rho_f}{\rho_{nf}\mu_f}, \theta = \frac{T-T_0}{T_0}, C = \frac{C'-C_0}{C_0}, \mathrm{Pr} = \frac{k_f(\rho C_p)_{nf}}{k_{nf}(\rho C_p)_f}$$

$$, Sc = \frac{k_f(\rho C_p)_{nf}}{D(\rho C_p)_f}, k_0 = \frac{k_r^2(\rho C_p)_f}{(\rho C_p)_{nf} v'^2}, M = \frac{\sigma B_0^2 \mu_{nf}\rho_f}{\mu_f \rho_{nf} {v_r}^2}, N = \frac{16\zeta T_0^3 \rho_f}{3\alpha(C_p)_{nf}},$$

$$Gr_\theta = \frac{g\beta_{nf}(T-T_0)\mu_{nf}}{v_0 u^2 \beta_f}, Gr_C = \frac{g\beta'_{nf}(C'-C_0)\mu_{nf}}{v_0 u^2 \beta'_f}, \chi = \frac{\upsilon\rho_f}{\rho_{nf}\kappa\mu_{nf}}$$

Rewriting equations (1) – (4) in dimensionless form, the modeled equations are transformed into

$$\frac{\partial}{\partial t}\left(\frac{\rho_{nf}}{\rho_f}\right) + \frac{1}{r}\frac{\partial}{\partial r}\left(\frac{\rho_{nf}}{\rho_f} ru\right) = 0 \tag{9}$$

$$\frac{\partial u}{\partial t} + u\frac{\partial u}{\partial r} = A_1 \mathrm{Re}^{-1}\left(\frac{\partial^2 u}{\partial r^2} + \frac{1}{r}\frac{\partial u}{\partial r} - \frac{u}{r^2}\right) + A_2 Gr_\theta \theta + A_3 Gr_C C - (\chi + M)A_4 u \tag{10}$$

$$\frac{\partial \theta}{\partial t} + u\frac{\partial \theta}{\partial t} = A_5 \mathrm{Pr}^{-1}\left(\frac{1}{r}\frac{\partial \theta}{\partial r} + \frac{\partial^2 \theta}{\partial r^2}\right) - A_6 N\theta \tag{11}$$

$$\frac{\partial C}{\partial t} + u\frac{\partial C}{\partial t} = A_6 Sc^{-1}\left(\frac{1}{r}\frac{\partial C}{\partial r} + \frac{\partial^2 C}{\partial r^2}\right) - A_6 k_0 C \tag{12}$$

Subject to the transformed boundary conditions $u(0,t)=0, u(1,t)=U$, $\theta(0,t)=1, \theta(\infty,0)=0$ $C(0,t)=1, C(\infty,t)=0$

where Re is Reynolds' number, Pr is Prandtl number, Sc is Schmidt number, Gr_θ is thermal Grashofs number, Gr_c is modified Grashofs number, N is dimensionless radiation term, θ is dimensionless temperature, u is dimensionless velocity, C is dimensionless concentration, χ is dimensionless porosity term, M is magnetic Hartmann number, k_0 is dimensionless chemical reaction term and r is dimensionless radius of nanoparticles.

$$A_1 = \frac{1+a\phi+b\phi^2}{1-\phi+\phi\frac{\rho_s}{\rho_f}},\ A_2 = 1-\phi+\phi\frac{\beta_s}{\beta_f},\ A_3 = 1-\phi+\phi\frac{\beta_s'}{\beta_f'},\ A_4 = \left(1-\phi+\phi\frac{\rho_s}{\rho_f}\right)^{-1}$$

$$A_5 = \left(\frac{k_s+(n-1)k_f+(n-1)(k_s-k_f)\phi}{k_s+(n-1)k_f-(k_s-k_f)\phi} + 5x10^4\,\xi\phi(\rho C_p)_s\sqrt{\frac{k_B T}{\rho_s D_s}}\,f(T,\phi)\right)\Big/\left(1-\phi+\phi\frac{(\rho C_p)_s}{(\rho C_p)_f}\right)$$

$$A_6 = \left(1-\phi+\phi\frac{(\rho C_p)_s}{(\rho C_p)_f}\right)^{-1}$$

III. METHOD OF SOLUTION

As a necessary condition and for science and engineering applications, it is assumed that the nanofluid is incompressible. Equation (9), therefore, takes the form

$$u = \frac{B}{r} \tag{13}$$

where B is integration constant.

In view of equation (13), equations (10) – (12) take the form

$$\frac{\partial u}{\partial t}+\frac{B}{r}\frac{\partial u}{\partial r} = A_1\,\mathrm{Re}^{-1}\left(\frac{\partial^2 u}{\partial r^2}+\frac{1}{r}\frac{\partial u}{\partial r}-\frac{u}{r^2}\right)+A_2 Gr_\theta\theta+A_3 Gr_C C-(\chi+M)A_4 u \tag{14}$$

$$\frac{\partial \theta}{\partial t}+\frac{B}{r}\frac{\partial \theta}{\partial t} = A_5\,\mathrm{Pr}^{-1}\left(\frac{1}{r}\frac{\partial \theta}{\partial r}+\frac{\partial^2\theta}{\partial r^2}\right)-A_6 N\theta \tag{15}$$

$$\frac{\partial C}{\partial t}+\frac{B}{r}\frac{\partial C}{\partial t} = A_6 Sc^{-1}\left(\frac{1}{r}\frac{\partial C}{\partial r}+\frac{\partial^2 C}{\partial r^2}\right)-A_6 k_0 C \tag{16}$$

Using the transformation technique adopted by Aaiza et al [38] and Ngiangia and Akaezue [39], a regular perturbation of the form

$$u(r,t) = u_0(r)+u_1(r)e^{i\omega t} \tag{17}$$

$$\theta(r,t) = \theta_0(r)+\theta_1(r)e^{i\omega t} \tag{18}$$

$$C(r,t) = C_0(r)+C_1(r)e^{i\omega t} \tag{19}$$

is chosen.

where ω is dimensionless free stream frequency.

Equation (19) is put into equation (16), equation (18) substituted into equation (15) and equations (17) – (19) is put into equation (14), the simplified equations result into

$$\frac{A_1}{\mathrm{Re}}u_1''(r)+\left(\frac{A_1}{r\,\mathrm{Re}}-\frac{B}{r}\right)u_1'(r)-\left(i\omega+A_4(\chi+M)+\frac{A_1}{\mathrm{Re}}\frac{1}{r^2}\right)u_1(r)+ \tag{20}$$

$$A_2 Gr_\theta\theta_1(r)+A_3 Gr_c C_1(r) = 0$$

$$\frac{A_1}{\mathrm{Re}}u_0''(r)+\left(\frac{A_1}{r\,\mathrm{Re}}-\frac{B}{r}\right)u_0'(r)-\left(A_4(\chi+M)+\frac{A_1}{\mathrm{Re}}\frac{1}{r^2}\right)u_0(r)+ \tag{21}$$
$$A_2Gr_\theta\theta_0(r)+A_3Gr_cC_0(r)=0$$

$$\frac{A_5}{\mathrm{Pr}}\theta_1''(r)+\left(\frac{A_5}{r\,\mathrm{Pr}}-\frac{B}{r}\right)\theta_1'(r)-(A_6N+i\omega)\theta_1(r)=0 \tag{22}$$

$$\frac{A_5}{\mathrm{Pr}}\theta_0''(r)+\left(\frac{A_5}{r\,\mathrm{Pr}}-\frac{B}{r}\right)\theta_0'(r)-(A_6N)\theta_0(r)=0 \tag{23}$$

$$\frac{A_6}{Sc}C_1''(r)+\left(\frac{A_6}{rSc}-\frac{B}{r}\right)C_1'(r)-(A_6k_0+i\omega)C_1(r)=0 \tag{24}$$

$$\frac{A_6}{Sc}C_0''(r)+\left(\frac{A_6}{rSc}-\frac{B}{r}\right)C_0'(r)-(A_6k_0)C_0(r)=0 \tag{25}$$

Subject to the modified boundary conditions $u_0(0,t)=0,u_0(1,t)=U$, $u_1(0,t)=0,u_1(1,t)=U$ $\theta_0(0,t)=1,\theta_0(\infty,0)=0$
$C_1(0,t)=1,C_1(\infty,t)=0$, $C_0(0,t)=1,C_0(\infty,t)=0$. Prime denotes derivative with respect to r

Equation (25) is tested and proved finite with the presence of singular point, hence analytic (Gupta [40], Raisinghania [41]), therefore, analytical feasible solution is possible. Using Frobenius method, a solution of the form

$$C_0(r)=\sum_{n=0}^{\infty}a_nr^{\lambda+\varepsilon} \tag{26}$$

is assumed.

The expression in equation (26) is substituted into equation (25) and after simplification, obtained an indicial equation of the form

$$\varepsilon^2-\left(\frac{ScB}{A_6}\right)\varepsilon=0 \tag{27}$$

is obtained with the solution as

$$\varepsilon=0 \quad \text{or} \quad \frac{ScB}{A_6} \tag{28}$$

The recursion formula is given by

$$a_\lambda=\frac{A_6Sck_0a_{\lambda-2}}{A_6(\lambda+\varepsilon)^2-ScB(\lambda+\varepsilon)} \qquad \lambda\geq 2 \tag{29}$$

and the solution after imposing the boundary conditions $C_0(0,t)=1,C_0(\infty,t)=0$
is given by

$$C_0(r)=1-\left(\frac{A_6Sck_0}{4A_6-2ScB}\right)r+\left(\frac{A_6Sck_0}{4A_6-2ScB}\right)r^2+..... \tag{30}$$

Using the same approach, the recurrence relation of equation (24) is given as

$$a_{\lambda} = \frac{\left(A_6 Sck_0 + i\omega Sc\right)a_{\lambda-2}}{A_6\left(\lambda+\varepsilon\right)^2 - ScB\left(\lambda+\varepsilon\right)} \qquad \lambda \geq 2 \qquad (31)$$

and solution after imposing the boundary conditions $C_1(0,t)=1, C_1(\infty,t)=0$ is

$$C_1(r) = 1 - \left(\frac{A_6 Sck_0 + i\omega Sc}{4A_6 - 2ScB}\right)r + \left(\frac{A_6 Sck_0 + i\omega Sc}{4A_6 - 2ScB}\right)r^2 + ... \qquad (32)$$

To determine the solution of equation (23), A_5, which Brownian motion is part, is temperature dependent, therefore, simplified to take the form

$$A_5 = a_1 A_6 + b_1 A_6 \theta^{1.5}(r) + A_6 c_1 \theta^{0.5}(r) \qquad (33)$$

$\theta^{1.5}(r)$ and $\theta^{0.5}(r)$ are approximated using Taylor's series expansion about 1 and neglect powers of $\theta(r) \geq 2$ and simplify, equation (23) can be written as

$$\left(\frac{\beta_1 + \beta_2\theta_0(r)}{\Pr}\right)\theta_0''(r) + \left(\frac{\beta_1 + \beta_2\theta_0(r)}{r\Pr} - \frac{B}{r}\right)\theta_0'(r) - A_6 N\theta_0(r) = 0 \qquad (34)$$

and its solution, taken $+ve\theta_0(r)$ is given as

$$\theta_0(r) = -\left(\frac{\beta_1 - A_6 \Pr Nr^2}{2\beta_2}\right) + \frac{1}{2}\sqrt{\left(\frac{\beta_1 - A_6 \Pr Nr^2}{\beta_2}\right)^2 + 4\left(\frac{\beta_1 + \beta_2}{\beta_2}\left(1 - r^2\right)\right)} \qquad (35)$$

where $\beta_1 = A_6\left(a_1 - \frac{b_1}{2} + \frac{c_1}{2}\right)$, $\beta_2 = \frac{A_6}{2}\left(3b_1 + c_1\right)$,

$$a_1 = \left(\frac{k_s + (n-1)k_f + (n-1)\left(k_s - k_f\right)\phi}{k_s + (n-1)k_f - \left(k_s - k_f\right)\phi} \Big/ \left(1 - \phi + \phi\frac{\left(\rho C_p\right)_s}{\left(\rho C_p\right)_f}\right)\right) ,$$

$$b_1 = 5x10^4\,\xi\phi\left(\rho C_p\right)_s\sqrt{\frac{k_B}{\rho_s D_s}}\left(-6.04\phi + 0.4705\right) \Big/ \left(1 - \phi + \phi\frac{\left(\rho C_p\right)_s}{\left(\rho C_p\right)_f}\right)$$

$$c_1 = 5x10^4\,\xi\phi\left(\rho C_p\right)_s\sqrt{\frac{k_B}{\rho_s D_s}}\left(1722.3\phi - 134.63\right) \Big/ \left(1 - \phi + \phi\frac{\left(\rho C_p\right)_s}{\left(\rho C_p\right)_f}\right)$$

Similarly, adopting the same method and procedure, the solution of equation (22) is therefore,

$$\theta_1(r) = -\left(\frac{\beta_1 - \left(A_6(N\Pr + i\omega)\right)r^2}{2\beta_2}\right) + \frac{1}{2}\sqrt{\left(\frac{\beta_1 - \left(A_6(N\Pr + i\omega)\right)r^2}{\beta_2}\right)^2 + 4\left(\left(\frac{\beta_1 + \beta_2}{\beta_2}\right)\left(1 - r^2\right)\right)} \qquad (36)$$

Binomial series expansion of the second term of equation (35) is carried out and terminated at r^2, the complete expression together with equation (30) is put into equation (21) and the result is given as

$$\frac{A_1}{\mathrm{Re}}u_0''(r)+\left(\frac{A_1}{r\,\mathrm{Re}}-\frac{B}{r}\right)u_0'(r)-\left(A_4(\chi+M)+\frac{A_1}{\mathrm{Re}}\frac{1}{r^2}\right)u_0(r)=$$

$$1-a_2r-\left(\frac{a_3}{2a_4}+a_5\right)r^2 \qquad (37)$$

The complete solution, which is a combination of the complimentary function and the particular integral after the imposition of the boundary conditions $u_0(0,t)=0, u_0(1,t)=U$

is

$$u_0(r)=a_6r^{\varepsilon_1}\left(1+a_7r^2\right)+a_8r^{1+\varepsilon_1}+a_6r^{\varepsilon_2}\left(1+a_9r^2\right)+a_8r^{1+\varepsilon_2}+a_{10}+a_{11}r+a_{12}r^2 \quad (38)$$

where

$$a_2=A_2Gr_c\left(1-\frac{A_6Sck_0}{4A_6-2ScB}\right) \qquad a_3=A_2Gr_\theta\left(\frac{2\beta_1A_6\,\mathrm{Pr}\,N}{\beta_2^2}+4\left(\frac{\beta_1+\beta_2}{\beta_2}\right)\right),$$

$$a_4=A_2Gr_\theta\left(\frac{\beta_1^2+4\beta_2(\beta_1+\beta_2)}{\beta_2^2}\right),\ a_5=A_2Gr_c\left(\frac{A_6Sck_0}{4A_6-2ScB}\right),$$

$$a_6=\frac{U-2-(a_{10}+a_{11}+a_{12})}{(1+a_7)(1+a_9)},\ a_7=\frac{\mathrm{Re}\,A_4(\chi+M)}{A_1(1+\varepsilon_1)(2+\varepsilon_1)-\mathrm{Re}\,B},$$

$$a_8=\frac{U-(1+a_7)(1+a_9)-(a_{10}-a_{11}-a_{12})}{2},a_9=\frac{\mathrm{Re}\,A_4(\chi+M)}{A_1(1+\varepsilon_2)(2+\varepsilon_2)-\mathrm{Re}\,B}$$

$$a_{10}=\frac{(a_3+2a_4a_5)(A_1-2\,\mathrm{Re}\,B)}{2a_4\,\mathrm{Re}(A_4(\chi+M))^2}-\frac{1}{A_4(\chi+M)},\ a_{11}=\frac{a_2}{A_4(\chi+M)},\ a_{12}=\frac{a_3+2a_4a_5}{2a_4A_4(\chi+M)}$$

$$\varepsilon_{1,2}=\frac{1\pm\sqrt{1+4\frac{B\,\mathrm{Re}}{A_1}}}{2}$$

Similarly, following the same method, series expansion of equation (36) is done together with equation (32) is put into equation (20) and the expression takes the form

$$\frac{A_1}{\mathrm{Re}}u_1''(r)+\left(\frac{A_1}{r\,\mathrm{Re}}-\frac{B}{r}\right)u_1'(r)-\left(i\omega+A_4(\chi+M)+\frac{A_1}{\mathrm{Re}}\frac{1}{r^2}\right)u_1(r)=$$

$$1-a_{22}r-\left(\frac{a_{33}}{2a_4}+a_{55}\right)r^2 \qquad (39)$$

and the complete solution is given as

$$u_1(r)=a_{66}r^{\varepsilon_1}\left(1+a_{77}r^2\right)+a_{88}r^{1+\varepsilon_1}+a_{66}r^{\varepsilon_2}\left(1+a_{99}r^2\right)+a_{88}r^{1+\varepsilon_2}+a_{20}+a_{21}r+a_{26}r^2 \quad (40)$$

where

$$a_{22} = A_2 Gr_c\left(1-\frac{A_6 Sck_0 + i\omega Sc}{4A_6 - 2ScB}\right),\ a_{33} = A_2 Gr_\theta\left(\frac{2\beta_1 A_6(\Pr N + i\psi)}{\beta_2^2} + 4\left(\frac{\beta_1+\beta_2}{\beta_2}\right)\right)$$

$$a_{55} = A_2 Gr_c\left(\frac{A_6 Sck_0 + i\omega Sc}{4A_6 - 2ScB}\right),\ a_{66} = \frac{U-2-(a_{20}+a_{21}+a_{26})}{(1+a_{77})(1+a_{99})}$$

$$a_{77} = \frac{\mathrm{Re}(i\omega + A_4(\chi+M))}{A_1(1+\varepsilon_1)(2+\varepsilon_1) - \mathrm{Re}\,B},\ a_{88} = \frac{U-(1+a_{77})(1+a_{99})-(a_{20}-a_{21}-a_{26})}{2}$$

$$a_{99} = \frac{\mathrm{Re}(i\omega + A_4(\chi+M))}{A_1(1+\varepsilon_2)(2+\varepsilon_2) - \mathrm{Re}\,B}, a_{20} = \frac{(a_{33}+2a_4a_{55})(A_1-2\,\mathrm{Re}\,B)}{2a_4\,\mathrm{Re}(i\omega + A_4(\chi+M))^2} - \frac{1}{i\omega + A_4(\chi+M)},$$

$$a_{21} = \frac{a_{22}}{i\omega + A_4(\chi+M)},\ a_{26} = \frac{a_{33}+2a_4a_{55}}{2a_4(i\omega + A_4(\chi+M))}$$

Finally, equations (38) and (40) is put into equation (17), equations (35) and (36) is put into equation (18) and equations (30) and (32) is put into equation (19) and the resulting expression takes the form

$$u(r,t) = a_6 r^{\varepsilon_1}\left(1+a_7 r^2\right) + a_8 r^{1+\varepsilon_1} + a_6 r^{\varepsilon_2}\left(1+a_9 r^2\right) + a_8 r^{1+\varepsilon_2} + a_{10} + a_{11} r + a_{12} r^2 +$$
$$\left(a_{66} r^{\varepsilon_1}\left(1+a_{77} r^2\right) + a_{88} r^{1+\varepsilon_1} + a_{66} r^{\varepsilon_2}\left(1+a_{99} r^2\right) + a_{88} r^{1+\varepsilon_2} + a_{20} + a_{21} r + a_{26} r^2\right) e^{i\omega t} \quad (41)$$

$$\theta(r,t) = -\left(\frac{\beta_1 - A_6 \Pr N r^2}{2\beta_2}\right) + \frac{1}{2}\sqrt{\left(\frac{\beta_1 - A_6 \Pr N r^2}{\beta_2}\right)^2 + 4\left(\frac{\beta_1+\beta_2}{\beta_2}\left(1-r^2\right)\right)} +$$
$$\left(-\left(\frac{\beta_1 - (A_6(N\Pr + i\omega))r^2}{2\beta_2}\right) + \right.$$
$$\left.\frac{1}{2}\sqrt{\left(\frac{\beta_1 - (A_6(N\Pr + i\omega))r^2}{\beta_2}\right)^2 + 4\left(\left(\frac{\beta_1+\beta_2}{\beta_2}\right)\left(1-r^2\right)\right)}\right) e^{i\omega t} \quad (42)$$

$$C(r,t) = 1 - \left(\frac{A_6 Sck_0}{4A_6 - 2ScB}\right) r + \left(\frac{A_6 Sck_0}{4A_6 - 2ScB}\right) r^2 + \ldots\ldots +$$
$$\left(1 - \left(\frac{A_6 Sck_0 + i\omega Sc}{4A_6 - 2ScB}\right) r + \left(\frac{A_6 Sck_0 + i\omega Sc}{4A_6 - 2ScB}\right) r^2 + \ldots\ldots\right) e^{i\omega t} \quad (43)$$

SPECIAL CASE

In the absence of Brownian motion $(A_5 = a_1)$, equations (41) and (42) reduced to

$$u(r,t) = a_{6+} r^{\varepsilon_1}\left(1+a_{7+} r^2\right) + a_{8+} r^{1+\varepsilon_1} + a_{6+} r^{\varepsilon_2}\left(1+a_{9+} r^2\right) + a_{8+} r^{1+\varepsilon_2} + a_{30} + a_{31} r + a_{32} r^2 +$$
$$\left(a_{66+} r^{\varepsilon_1}\left(1+a_{77+} r^2\right) + a_{88+} r^{1+\varepsilon_1} + a_{66+} r^{\varepsilon_2}\left(1+a_{99+} r^2\right) + a_{88+} r^{1+\varepsilon_2} + a_{40} + a_{41} r + a_{42} r^2\right) e^{i\omega t} \quad (44)$$

$$\theta(r,t) = 1 - \left(\frac{a_1 \Pr N}{4a_1 - 2\Pr B}\right) r + \left(\frac{a_1 \Pr N}{4a_1 - 2\Pr B}\right) r^2 + ... +$$

$$(1 - \left(\frac{a_1 \Pr N + i\omega \Pr}{4a_1 - 2\Pr B}\right) r + \left(\frac{a_1 \Pr N + i\omega \Pr}{4a_1 - 2\Pr B}\right) r^2 + ...) e^{i\omega t} \quad (45)$$

where

$$a_{30} = \frac{\left(A_2 Gr_\theta + A_3 Gr_c\right) + \left(\frac{3A_1 - 2\,\mathrm{Re}\, B}{\mathrm{Re}}\right) a_{31}}{A_4(\chi + M)} \quad a_{31} = \frac{A_2 Gr_\theta \left(\frac{a_1 \Pr N}{4a_1 - 2\Pr B}\right) + A_3 Gr_c \left(\frac{A_6 Sck_0}{4A_6 - 2ScB}\right)}{A_4(\chi + M)} = a_{32},$$

$$a_{40} = \frac{\left(A_2 Gr_\theta + A_3 Gr_c\right) + \left(\frac{3A_1 - 2\,\mathrm{Re}\, B}{\mathrm{Re}}\right) a_{31}}{A_4(\chi + M) + i\omega}, a_{41} = \frac{A_2 Gr_\theta \left(\frac{a_1 \Pr N + i\omega \Pr}{4a_1 - 2\Pr B}\right) + A_3 Gr_c \left(\frac{A_6 Sck_0 + i\omega Sc}{4A_6 - 2ScB}\right)}{A_4(\chi + M) + i\omega} = a_{42}$$

$$a_{6+} = \frac{U - (a_{30} - a_{31} - a_{32})(A_1(\varepsilon_1 + 1)(\varepsilon_2 + 2) - \mathrm{Re}\, B)}{(A_1(\varepsilon_1 + 1)(\varepsilon_1 + 2) - \mathrm{Re}\, B) + (\mathrm{Re}(A_4(\chi + M))}$$

$$a_{7+} = \frac{\mathrm{Re}(A_4(\chi + M))}{A_1(\varepsilon_1 + 1)(\varepsilon_1 + 2) - \mathrm{Re}\, B}, \; a_{8+} = (U - (a_{30} - a_{31} - a_{32}))$$

$$a_{9+} = \frac{\mathrm{Re}(A_4(\chi + M))}{A_1(\varepsilon_2 + 1)(\varepsilon_2 + 2) - \mathrm{Re}\, B}$$

$$a_{66+} = \frac{U - (a_{40} - a_{41} - a_{42})(A_1(\varepsilon_1 + 1)(\varepsilon_2 + 2) - \mathrm{Re}\, B)}{(A_1(\varepsilon_1 + 1)(\varepsilon_1 + 2) - \mathrm{Re}\, B) + (\mathrm{Re}(A_4(\chi + M) + i\omega)}$$

$$a_{77+} = \frac{\mathrm{Re}(A_4(\chi + M) + i\omega)}{A_1(\varepsilon_1 + 1)(\varepsilon_1 + 2) - \mathrm{Re}\, B}, \; a_{88+} = (U - (a_{40} - a_{41} - a_{42}))$$

$$a_{99+} = \frac{\mathrm{Re}(A_4(\chi + M) + i\omega)}{A_1(\varepsilon_2 + 1)(\varepsilon_2 + 2) - \mathrm{Re}\, B}$$

The mass flux ϖ, the mean temperature θ_m and the mean specie concentration C_m are obtained by evaluating the integrals

$$\varpi = \int_0^1 u(r,t)dr \quad (46)$$

$$\theta_m = \frac{\int_0^1 u(r,t)\theta(r)dr}{\int_0^1 u(r,t)dr} \quad (47)$$

and

$$C_m = \frac{\int_0^1 u(r,t)C(r)dr}{\int_0^1 u(r,t)dr} \tag{48}$$

IV. SKIN FRICTION (τ), NUSSELT NUMBER (Nu) AND SHERWOOD NUMBER (Sh)

The shearing stress, Nusselt number and Sherwood number are applicable physical parameters worthy of mention in nanofluids flow through concentric cylindrical surfaces in porous medium.

Skin Friction

The skin friction is given by

$$\left.\frac{\partial u(r,t)}{\partial r}\right|_{r=0} = a_{11} + a_{21} \tag{49}$$

Heat Transfer Coefficient or Nusselt Number (Nu)

Literatures have shown that the heat transfer coefficient or Nusselt number is a better indicator than the effective thermal conductivity of nanofluids, particularly when such nanofluids are used as coolants and other functions in industries, in the determination of the effect of temperature on nanofluids. Taking the Taylor series expansion of equation (42) about the point $r = 1$ and neglecting powers of $r > 1$, it is determined as

$$\left.\frac{\partial \theta(r,t)}{\partial r}\right|_{r=0} = Nu = \frac{2A_6 \Pr N}{\beta_2} - 2\frac{\beta_2\left(\frac{A_6 \Pr N}{\beta_2}\right)^2}{\beta_1} - 8\left(\frac{\beta_1+\beta_2}{\beta_2}\right) + \left(2\left(\frac{A_6(\Pr N + i\omega)}{\beta_2}\right) - 2\frac{\beta_2\left(\frac{A_6(\Pr N + i\omega)}{\beta_2}\right)^2}{\beta_1} - 8\left(\frac{\beta_1+\beta_2}{\beta_2}\right)\right)e^{i\omega t} \tag{50}$$

Mass Transfer Coefficient or Sherwood Number (Sh)

The Sherwood number is calculated thus,

$$\left.\frac{\partial C(r,t)}{\partial r}\right|_{r=0} = Sh = \left(\frac{A_6 Sck_0}{4A_6 - 2ScB}\right) + ... \left(\left(\frac{A_6 Sck_0 + i\omega Sc}{4A_6 - 2ScB}\right) + ..\right)e^{i\omega t} \tag{51}$$

Special case

In the absence of Brownian motion $(A_5 = a_1)$, equations (44) and (45) reduced to the form

$$\left.\frac{\partial u(r,t)}{\partial r}\right|_{r=0} = \tau = a_{31} + a_{41} \tag{52}$$

$$\left.\frac{\partial \theta(r,t)}{\partial r}\right|_{r=0} = Nu = \left(\frac{a_1 \Pr N}{4a_1 - 2\Pr B}\right) + ... \left(\left(\frac{a_1 \Pr N + i\omega \Pr}{4a_1 - 2\Pr B}\right) + ...\right)e^{i\omega t} \tag{53}$$

V. RESULTS AND DISCUSSIONS

Results

In order to get physical insight and numerical validation of the problem, an approximate value of $Ds = 0.015nm, \xi = t = B = U = 1, k_B = 1.380658x10^{-23} JK^{-1}$ are chosen. The values of other parameters made use of are

$$\text{Re} = 100,200,300,.400, Gr_\theta = 1.35,2.35,3.35,4.35, M = 0.47,1.47,2.47,3.47$$
$$k_0 = 0.51,0.81,1.11,1.41, \Pr = 0.71,0.81,0.91,1.01, N = 1.62,1.72,1.82,1.92$$
$$Gr_c = 1.02,2.02,3.02,4.02, \phi = 0.03,0.05,0.07,0.09, Sc = 2.15,3.15,4.15,5.15$$
$$\omega = 2.3,3.3,4.3,5.3, \chi = 0.01,0.04,0.07,0.10$$

Table 1: Sphericity ψ and empirical shape factor n for nanoparticles (Aaiza et al [38])

Model	Cylinder
ψ	0.62
n	4.83871

Table 2: Constants **a** and **b** empirical shape factor (Aaiza et al [38])

Model	Cylinder
a	13.5
b	904.4

Table 3: Thermo physical properties of Cu nanoparticles and H_2O (Aaiza et al [38])

Property	H_2O	Cu
$(C_p)_{nf}$ (J/kgK)	4179	385
ρ (kg/m^3)	997.1	8933
k_{nf} (W/mk)	0.613	401
$\mu_{nf}\ (m^2 s^{-1})$	0.00089	0.00046
$\beta\ x10^{-5}(k^{-1})$	21	1.67

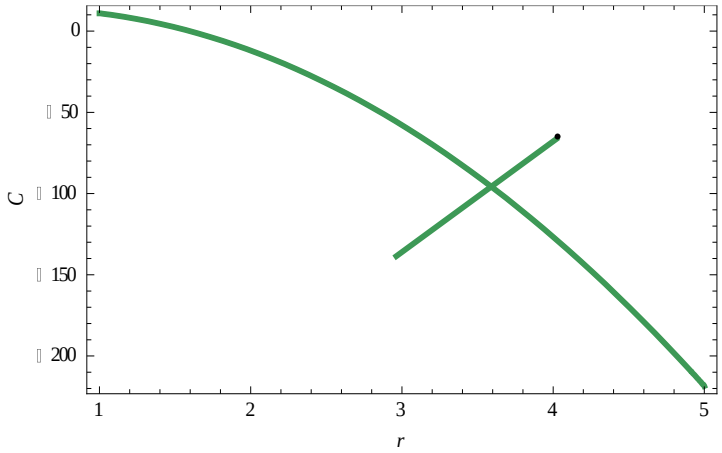

Fig. 1: **Concentration profile C against boundary layer r for varying chemical reaction k_0**

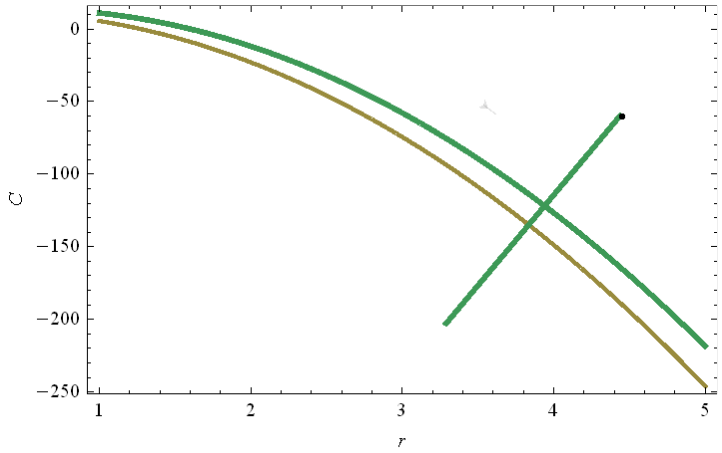

Fig. 2: **Concentration profile C against boundary layer r for varying Schmidt number Sc**

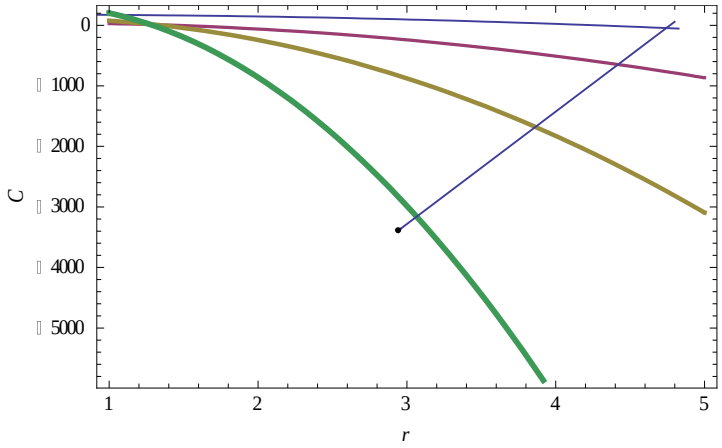

Fig. 3: **Concentration profile C against boundary layer r for varying free stream frequency ω**

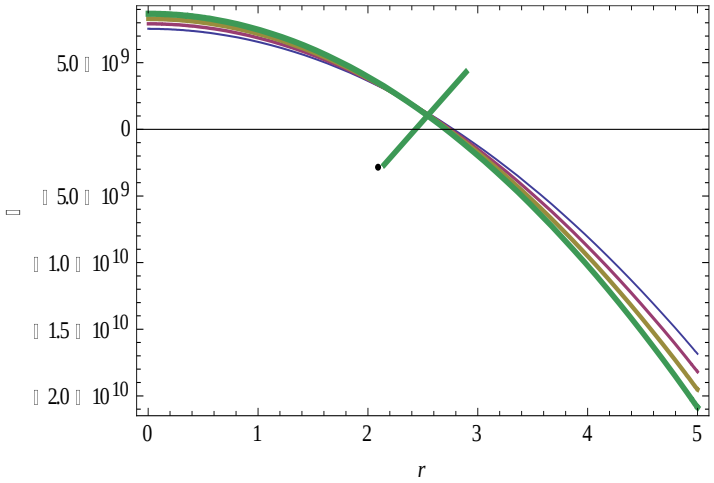

Fig. 4: **Temperature profile θ against boundary layer r for varying Prandtl number Pr**

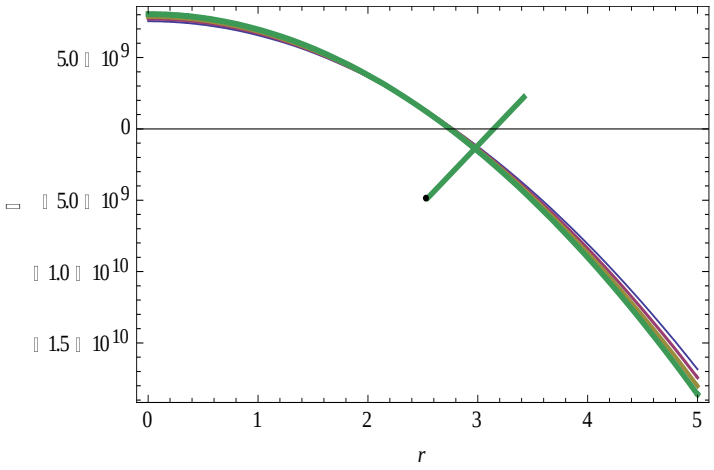

Fig. 5: **Temperature profile θ against boundary layer r for varying Radiation term N**

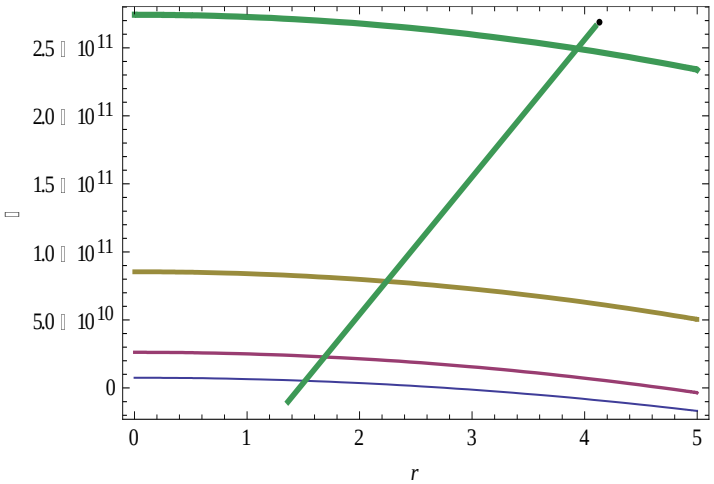

Fig. 6: **Temperature profile θ against boundary layer r for varying free stream frequency ω**

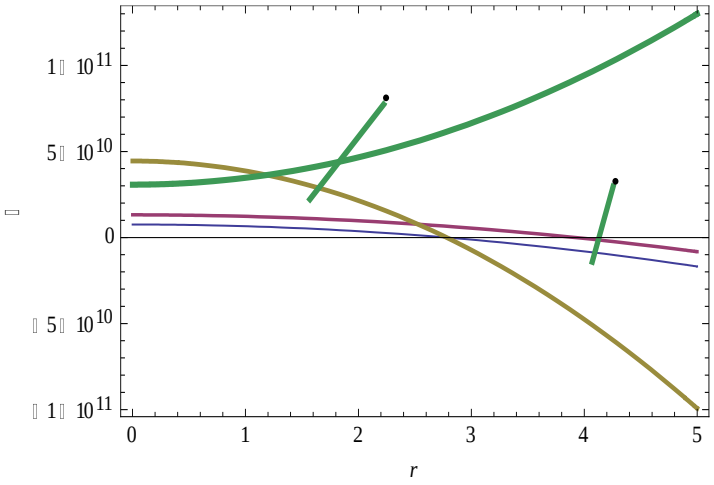

Fig. 7: **Temperature profile θ against boundary layer r for varying Nanoparticle volume fractions ϕ**

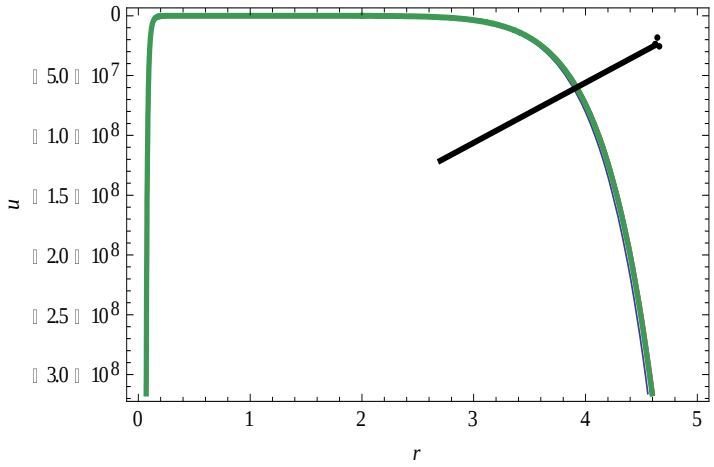

Fig. 8: **Velocity profile u against boundary layer r for varying permeability term χ**

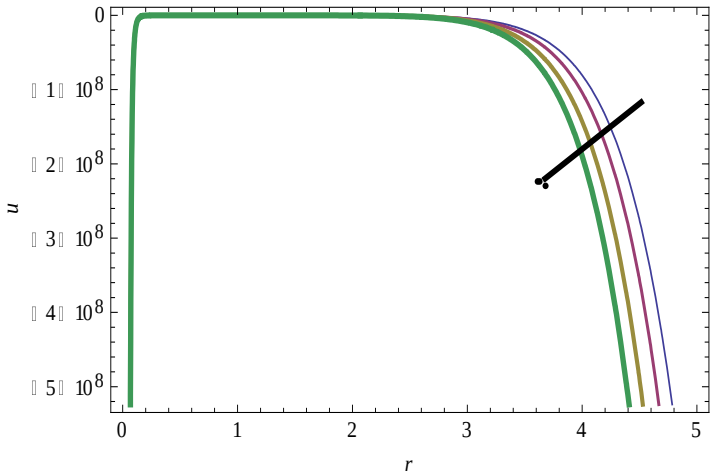

Fig. 9: **Velocity profile u against boundary layer r for varying Hartmann number M**

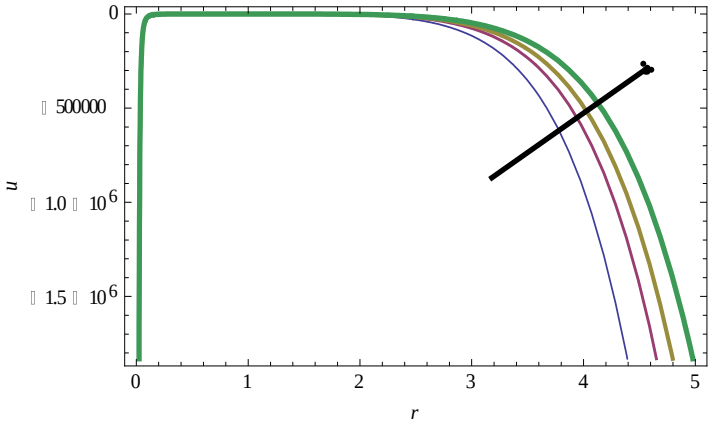

Fig. 10: **Velocity profile u against boundary layer r for varying nanoparticle volume fractions ϕ**

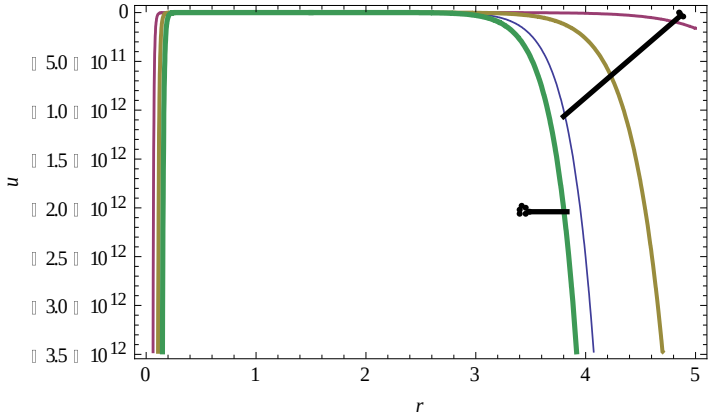

Fig. 11: **Velocity profile u against boundary layer r for varying Reynolds number** Re

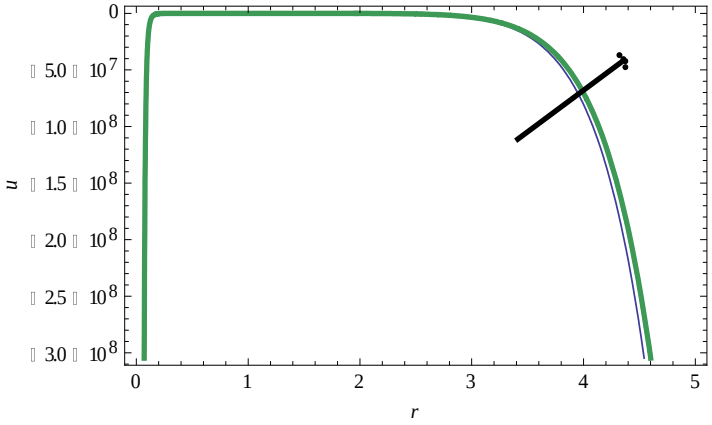

Fig. 12: **Velocity profile u against boundary layer r for varying Prandtl number** Pr

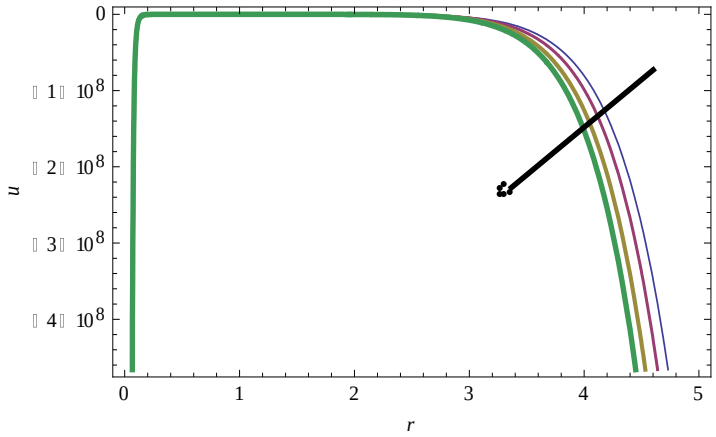

Fig. 13: **Velocity profile** u **against boundary layer** r **for varying free stream frequency** ω

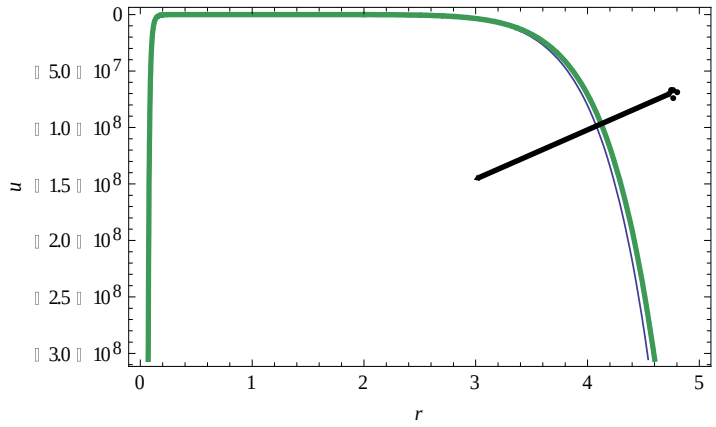

Fig. 14: **Velocity profile** u **against boundary layer** r **for varying radiation term** N

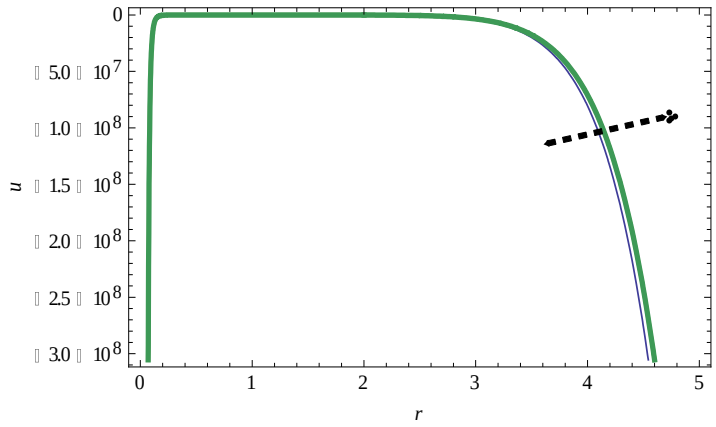

Fig. 15: **Velocity profile** u **against boundary layer** r **for varying Schmidt number** Sc

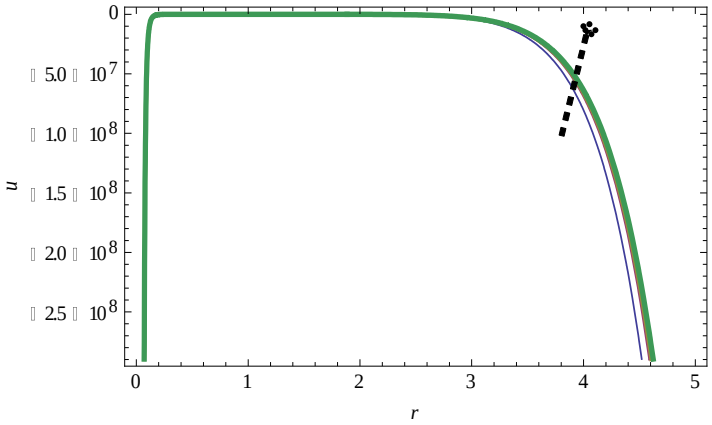

Fig. 16: Velocity profile u against boundary layer r for varying modified Grashof number Gr_c

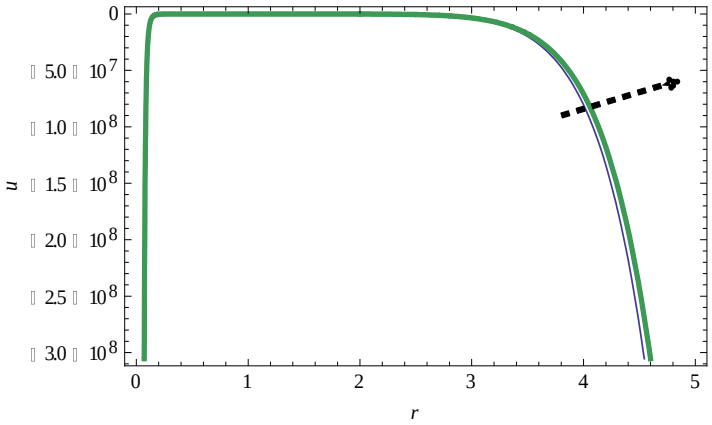

Fig. 17: Velocity profile u against boundary layer r for varying thermal Grashof number Gr_θ

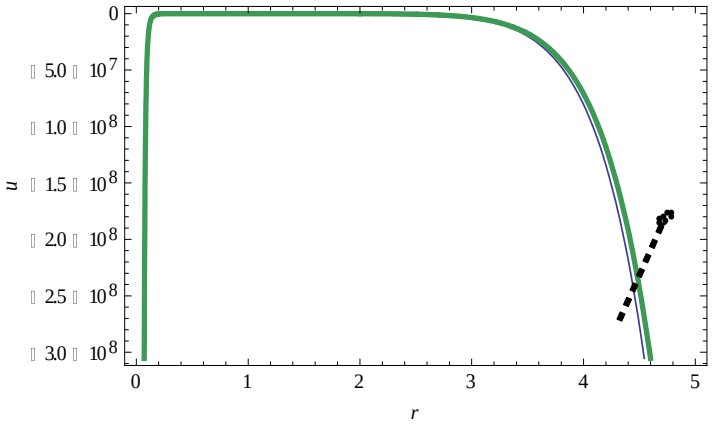

Fig. 18: Velocity profile u against boundary layer r for varying chemical reaction term k_0

Table 4: Numerical values of mean Nusselt number for various values of Prandtl number

Pr	Nu(Presence of Brownian motion)	Nu (Absence of Brownian motion)
0.71	-9073.28	9.65906

0.81	-9709.87	11.7557
0.91	-10346.50	14.1526
1.01	-10983.00	16.9191

Table 5: Numerical values of mean Nusselt number for various values of nanoparticles volume fractions ϕ

$\phi(nm^3)$	Nu(Presence of Brownian motion)	Nu(Absence of Brownian motion)
0.03	-9073.28	9.65906
0.05	-9200.79	8.88206
0.07	-9510.03	8.24468
0.09	-25307.80	7.71255

Table 6: Numerical values of mean Nusselt number for various values of radiations (N)

N	Nu(Presence of Brownian motion)	Nu(Absence of Brownian motion)
1.62	-9073.28	9.65906
1.72	-9352.28	9.94046
1.82	-9631.27	10.2219
1.92	-9910.27	10.5033

Table 7: Numerical values of mean Nusselt number for various values of free stream frequency ω

ω	Nu(Presence of Brownian motion)	Nu(Absence of Brownian motion)
2.3	9073.28	9.65906
3.3	-11038.10	31.5701
4.3	-13002.80	101.488
5.3	-14967.60	319.699

Table 8: Numerical values of skin friction for various values of free stream frequency (ω **)**

ω	τ (Presence of Brownian motion)	τ (Absence of Brownian motion)
2.3	3.35317	0.308809
3.3	3.27248	-0.0311142
4.3	3.22621	-0.371037
5.3	3.19622	-0.71096

Table 9: Numerical values of skin friction for various values of nanoparticle volume fractions ($\phi(nm^3)$)

$\phi(nm^3)$	τ (Presence of Brownian motion)	τ (Absence of Brownian motion)
0.03	3.35317	0.308809
0.05	3.62573	-0.0292914
0.07	3.88231	-0.342038
0.09	4.1247	-0.635677

Table 10: Numerical values of skin friction for various values of modified Grashof number (Gr_c)

Gr_c	τ (Presence of Brownian motion)	τ (Absence of Brownian motion)
1.02	3.35317	0.308809
2.02	6.64059	-2.60943
3.02	9.92801	-4.58319
4.02	13.2154	-6.55695

Table 11: Numerical values of skin friction for various values of thermal Grashof number (Gr_θ)

Gr_θ	τ (Presence of Brownian motion)	τ (Absence of Brownian motion)
1.35	--	0.308809
2.35	--	0.189323
3.35	--	1.49443
4.35	--	2.79953

Table 12: Numerical values of skin friction for various values of Prandtl number

Pr	τ (Presence of Brownian motion)	τ (Absence of Brownian motion)
0.71	--	0.308809
0.81	--	-0.733334
0.91	--	-0.296126
1.01	--	0.208513

Table 13: Numerical values of skin friction for various values of radiations (N)

N	τ (Presence of Brownian motion)	τ (Absence of Brownian motion)
1.62	--	0.308809
1.72	--	-1.04846
1.82	--	-0.981135
1.92	--	-0.913812

Table 14: Numerical values of skin friction for various values of Schmidt number (Sc)

Sc	τ (Presence of Brownian motion)	τ (Absence of Brownian motion)
2.15	3.35317	0.308809
3.15	3.35317	-1.11578
4.15	3.35317	-1.11578
5.15	3.35317	-1.11578

Table 15: Numerical values of skin friction for various values of chemical reaction (k_0)

k_0	τ (Presence of Brownian motion)	τ (Absence of Brownian motion)
0.51	3.35317	0.308809
0.81	3.35317	-1.11578
1.11	3.35317	-1.11578
1.41	3.35317	-1.11578

Table 16: Numerical values of skin friction for various values of porosity term (χ)

χ	τ (Presence of Brownian motion)	τ (Absence of Brownian motion)
0.01	3.35317	--
0.04	3.19551	--
0.07	3.05471	--
0.10	2.92812	--

Table 17: Numerical values of skin friction for various values of Hartmann number (χ)

M	τ (Presence of Brownian motion)	τ (Absence of Brownian motion)
0.47	3.35317	--
1.47	1.44036	--
2.47	0.991113	--
3.47	0.770432	--

Table 18: Numerical values of Sherwood number for various values of chemical reaction (k_0), Schmidt number (Sc **)** and free stream frequency (ω **)**

k_0	**Sh**	Sc	**Sh**	ω	**Sh**
0.51	-11.4703	2.15	-11.4703	2.3	-11.4703
0.81	-11.4703	3.15	-11.4703	3.3	-44.736
1.11	-11.4703	4.15	-11.4703	4.3	-158.455
1.41	-11.4703	5.15	-11.4703	5.3	-530.894

DISCUSSION

Chemical reaction influence is discussed in **Fig.1**. Increase in chemical reaction rate of the nanofluid, enhances the concentration.

Fig.2 presents the impact of Schmidt number on the concentration of the nanofluid. It is observed that an increase in the Schmidt number, showes a corresponding increase in the concentration of the copper nanofluid.

Free stream frequency effect as shown in **Fig.3**, revealed that its increase, enhances the concentration of the nanofluid.

Prandtl number influence is depicted in **Fig.4**. An increase in Prandtl number corresponds to a decrease in the temperature profile of the nanofluid. The reason is that, values of Prandtl number less than 1 of nanofluid is highly conductive.

Fig.5 illustrates the effect of the radiation parameter on the temperature profile of the nanofluid. It is observed that increase in radiation leads to lower temperature of the nanofluid.

Increase in the free stream frequency is associated with an increase in the temperature profile of the nanofluid and this effect is illustrated in Fig.6.

One of the important considerations in the description of nanofluid is the nanoparticle volume fraction. It influences almost all nanofluid parameters. Fig.7, shows that, increase in nanoparticle volume fraction corresponds to an increase in temperature profile caused by increased concentration of the copper nanofluid.

The effect of porosity on the velocity profile of the nanofluid is shown in **Fig.8**. It is noticed that an increase in porosity leads to an increase in velocity profile of the copper nanofluid. This is, as a result of increase in size of pore spaces of the porous medium.

Fig.9 portrays the influence of magnetic Hartmann number on the velocity profile. It is observed that the velocity profile of the nanofluid decreases with an increasing Hartmann number. The magnetic Hartmann number is a resistive force or Lorentz force on the fluid flow and reduces the motion of electrically conducting fluid.

The nanoparticle volume fraction is a distinguishing factor between ordinary fluid and nanofluid description. As observed in **Fig.10**, its increase, leads to a corresponding increase in the velocity profile of the copper nanofluid.

The Reynolds number range serves as a guide or describes the transition from Newtonian fluid to non-Newtonian fluid owing to increase viscosity. As shown in **Fig.11**, initial increase in Reynolds number $(\mathrm{Re} \le 300)$ results in an increase in the velocity profile but suddenly starts to decrease as Reynolds number is increased beyond 300, meaning increased viscosity and buttress the fact that the copper nanofluid has moved into the non-Newtonian domain when the Reynolds number is still within the Newtonian domain $(1 \le \mathrm{Re} \le 3000)$. This early onset of transition is a vital characteristic of copper nanofluid.

Copper nanofluid possesses abnormal high conductivity, it is therefore not surprising that an increase in Prandtl number as shown in Fig.12, corresponds to an increase in the velocity profile of the fluid.

Fig.13 reveals that an increase in free stream frequency of the nanofluid leads to a decrease in the velocity profile of the nanofluid.

As depicted in **Fig.14**, the nanofluid is warmth as a result of radiation and the resultant effect is increase in the velocity of the fluid.

Fig.15 shows that an increase in Schmidt number results to an increase in molecular diffusivity which leads to an increase in the velocity profile of the nanofluid.

Fig.16 and Fig.17 displayed the effect of thermal Grashof number and modified Grashof number respectively on the velocity profile of the nanofluid. Increase in thermal Grashof number (Gr_θ) means cooling the cylindrical plates while increase in modified Grashof number (Gr_c) means lowering the concentration of the nanofluid around the plates and both effects increase the velocity profile of the fluid.

Increase in the chemical reaction term as depicted in Fig.18, results in a gradual increase in the velocity profile of the fluid due to the reaction rate.

Tables 4, 6 and 7 showed numerical values of Nusselt numbers in the presence and absence of Brownian motion. As increase in the Prandtl number, radiation and free stream frequency correspond to decreasing Nusselt number in the presence of Brownian motion while an increase is observed when Brownian motion is not involved.

According to **Table 5**, increase in the nanoparticle volume fraction, decreases the Nusselt number in both the presence and absence of Brownian motion.

The free stream frequency, decreases the skin friction in the presence and absence of Brownian motion an illustrated in **Table 8**.

Tables 9 and 10 displayed that nanoparticle volume fraction and modified Grashof number, increased as the skin friction increases in the presence of Brownian motion but decreased in the absence of Brownian motion.

According to **Table 11**, the skin friction increases in the absence of Brownian motion but not applicable to the presence of Brownian motion.

Tables 12 and 13 showed that skin friction is not applicable in the presence of Brownian motion but decreases in the absence of Brownian motion for corresponding increases in Prandtl number and radiation term.
Marginal decrease is observed in both the presence and absence of Brownian motion in the skin friction as Schmidt number and chemical reaction term increases as shown in **Tables 14 and 15**.
Tables 16 and 17 revealed that decrease in skin friction is observed in the presence of Brownian motion but not applicable in the absence of Brownian motion as the magnetic Hartmann number and porosity increases.
Table 18 illustrates that; the Sherwood number decreases as approximation extends up to 8 decimal places when chemical reaction term and Schmidt number increases but decreases as free stream frequency increases.

VI. CONCLUSION

The approximate analytical solution to copper nanofluid in Couette flow regime with the effect of magnetic field and modified model for thermal conductivity is the kernel of this work. The key findings are that the effect of nanoparticle volume fractions and that of Brownian motion cannot be over emphasized. The transition of the copper nanofluid from Newtonian fluid to non-newtonian fluid domain when the Reynolds number increase is still within the laminar flow range is one important characteristics of copper nanofluid.

ACKNOWLEDGEMENT

The authors appreciate the effort of some of our colleagues that encouraged us to bring the work to fruition.

REFERENCES

[1] S. U. S Choi, Enhancing thermal conductivity of fluids with nanoparticle, in: D.A. Siginer, H.P. Wang (Eds.), Developments and Applications of Non-Newtonian Flows. ASME FED.66 (1995), 99–105
[2] K. V. Wong, O. Deleon. Applications of nanofluids: Current and future, Advances in Mechanical Engineering 2 (2010), 519659
[3] A. K Singh, G. Harinadha, N. Kishore, P. Barua, T. Jain, P. Joshi. Mixed Convective Heat Transfer Phenomena of Circular Cylinders to Non-Newtinian Nanofluids Flowing Upward. Procedia Engineering 127 (2015), 118-125
[4] P. W Bearman, M. M Zdravkovich, Flow around a circular cylinder near a plane boundary, Journal of Fluid Mechanics 89 (1978), 33-47
[5] S. Taniguchi, K. Miyakochi, Fluctuating fluid forces acting on a circular cylinder and interference with a plane wall, Experiments in Fluids 9 (1990), 197-204
[6] C. F Lange, F. Durst, M. Breuer, Momentum and heat transfer from cylinders in laminar cross flow at $104 \leq \mathrm{Re} \leq 200$, International Journal of Heat and Mass Transfer 410 (1998), 3409-3430
[7] M. Narahari, N. Alaparthi, I. Pop, Exact analysis of the transient free convection flow of nanofluids between two vertical parallel plates in the presence of radiation, (2017) https://doi.org/10.1002/cjce.22872
[8] W. A. Azhar, D. Vieru, C. Fetecau, Free convection flow of some fractional nanofluids over a moving vertical plate with uniform heat flux and hear source, Physics of Fluids 29 (2017), 082001
[9] A. K. Santra, S. Sen, N, Chakraborthy, Study of heat transfer due to laminar flow of copper-water nanofluid through two isothermally heated parallel plates, International Journal of Thermal Science 48 (2009), 391-400
[10] S. Sandip, G. Suvankar, D. Amaresh, Buoyancy driven flow and heat transfer of nanofluids past a square cylinder in vertically upward flow, International Journal of Heat and Mass Transfer 59 (2013), 433-450
[11] N. Ahmed, N. A. Shah, B. Ahmad, S. I. A. Shah, S. Ulhaq, M. Rahimi-Gorji, Transient MHD convective flow of fractional nanofluid between vertical plates, Journal of Applied Computational Mechanics 5(4) (2019) 592-602
[12] M. Turkyilmazoglu, Analytical solutions of single and multi phase models for the condessation of nanofluid film flow and heat transfer, European Journal of Mechanics-B/Fluids 53 (2015) 272-277
[13] P. Loganathan, P. N. Chand, P. Ganesan, Transient natural convective flow of a nanofluid past a vertical plate in the presence of heat generation, Journal of Applied Mechanics and Technology Physics 56 (2015), 433-442
[14] A. Hajizadeh, N. A. Shah, S. I. A. Shah, I. L. Animasaun, M. Rahimi-Gorji, I. M. Alarifi, Free convection flow of nanofluids between two vertical plates with thermal damp flux, Journal of Molecular Liquids 289 (2019), 110964
[15] Y. R. O. Reddy, M. S. Reddy, P. S. Reddy, A. J. Chamkha, Effect of Brownian motion and thermophoresis on heat and mass transfer flow over a horizontal circular cylinder filled with nanofluid, Journal of nanofluids 6(4) (2017), 702-710
[16] G. Sucharitha, S. Sreenadh, P. Lakshminarayana, K. Sushma, Brownian motion and thermophoresis effects on peristaltic slip flow of a MHD nanofluid in a symmetric/asymmetric channel, Materials Science and Engineering 263 (2017), 062025
[17] R. Kandasamy, I. Muhaimin, R. Mohamad, Thermophoresis and Brownianmotion effects on MHD boundary-layer flow of a nanofluid in the presence of thermal stratification due to solar radiation, Int. J. Mech. Sci. 70 (2013) 146–154, https://doi.org/10.1016/j.ijmecsci.2013.03.007.
[18] N. Anbuchezhian, K. Srinivasan, K. Chandrasekaran, R. Kandasamy, Thermophoresis and Brownian motion effects on boundary layer flow of nanofluid in presence of thermal stratification due to solar energy, Appl. Math. Mech. 33 (6) (2012) 765–780, https://doi.org/10.1007/s10483-012-1585-8.
[19] Y. Xuan, Q. Li, and W. Hu, Aggregation structure and thermal conductivity of nanofluids. AIChE Journal, (2003). 49(4), 1038–1043
[20] S. K. Das, N. Putta, P.Thiesen, and W. Roetzel, Temperature dependence of thermal conductivity enhancement for nanofluids. ASME Transnational Journal of Heat Transfer, (2003). 125, 567–574
[21] D. H. Kumar, H. E.Patel, V. R. R. Kumar, T Sundararajan, T. Pradeep, and S. K. Das, Model for heat conduction in nanofluids. Physical Review Letters, (2004). 93(14): 144,301–1–144,301–4
[22] P. Bhattacharya, S. K. Saha, A. Yadav, P. E. Phelan, and R. S. Prasher, Brownian dynamics simulation to determine the effective thermal conductivity of nanofluids. Journal of Applied Physics, (2004). 95(11): 6492–6494
[23] N. B. Reddy, T. Poornima, P. Sreenivasulu, Radiative heat transfer effect on MHD slip flow of dissipating nanofluid past an exponential stretching porous sheet, International Journal of Pure and Applied Mathematics 109 (9) (2016) 134–142

[24] P. Sreenivasulu, T. Poornima, N. Bhaskar Reddy, Thermal radiation effects on MHD boundary layer slip flow past a permeable exponential stretching sheet in the presence of joule heating and viscous dissipation, Journal of Applied Fluid Mechanics 9(1) (2016) 267–278.
[25] M. Tamoor, MHD convective boundary layer slip flow and heat transfer over nonlinearly stretching cylinder embedded in a thermally stratified medium, Results in Physics 7 (2017) 4247–4252, https://doi.org/10.1016/j.rinp.2017.07.064.
[26] S. K. Parida, S. Panda, B. R. Rout, MHD boundary layer slip flow and radiative nonlinear heat transfer over a flat plate with variable fluid properties and thermophoresis, Alexandria Engineering Journal 54 (4) (2015) 941–953, https://doi.org/10.1016/j.aej.2015.08.007.
[27] M. K. Nayak , Shaw S., Chamkha A.J, Impact of variable magnetic field and convective boundary condition on a stretched 3D radiative flow of Cu-H2O nanofluid, AMSE Journals-AMSE IIETA Publication-2017-Series: Modelling B; 86, 3, 2018, 658–678.
[28] Z. Abbas, M. Naveed, M. Sajid, Hydromagnetic slip flow of nanofluid over a curved stretching surface with heat generation and thermal radiation, Journal of molecular Liquids 215 (2016) 756–762
[29] B. Souayeh, M. G. Reddy, P. Sreenivasulu, T. Poornima, M. Rahimi-Gorji, I.M. Alarifi, Comparative analysis on non-linear radiative heat transfer on MHD Casson nanofluid past a thin needle, Journal of Molecular Liquids 284 (2019) 163–174
[30] A. T. Ngiangia, M.A Orukari MHD Couette-Poiseuille Flow in a Porous Medium, Global Journal of Pure and Applied Mathematics. 9(2) (2013), 169-181
[31] A. C. Cogley, A. W. Vincenti, E. S. Giles, . Differential Approximation of a Radiative Heat Transfer. The American Institute of Aeronautics and Astronautics. 6 (1968), 551–553
[32] R. L. Hamilton, O. K. Crosser, Thermal conductivity of heterogeneous two component systems. Industrial Engineering and Chemistry Fundamentals 1(3) (1962), 187-191.
[33] J. Koo, C. Kleinstreuer, A new thermal conductivity model for nanofluids. Journal of Nanoparticle Research, 6(6) (2004), 577–588
[34] J. Koo, C. Kleinstreuer, Laminar nanofluid flow in micro-heat sinks. International Journal of Heat and Mass Transfer, 48(13): (2005), 2652–2661
[35] A. T. Ngiangia, P. O. Nwabuzor, Investigation of Heat Transfer Characteristics of Spherical Copper and Alumina Nanoparticles in Water and Ethylene glycol Based Fluids, (Submitted)
[36] R. K, Tiwari, M. K. Das, Heat transfer augmentation in a two-sided lid-driven differentially heated square cavity utilizing nanofluids. International Journal of Heat and Mass Transfer. 50 (2007), 9-10.
[37] K. Asma, I. Khan, S. Sharidan, Exact solution for free convecton flow of nanofluids with ramped wall temperature. The European Physical Journal-Plus 130 (2015), 57-71.
[38] G. Aaiza, I. Khan, S. Shafie Energy transfer in mixed convection MHD flow of nanofluid containing different shapes of nanoparticles in a channel filled with saturated porous medium. Nanoscale Research Letters. 10 (490) (2015). 1-14.
[39] A.T. Ngiangia, N. N. Akaezue, Heat Transfer of Mixed Convection Electroconductivity Flow of Copper Nanofluid with Different Shapes in a Porous Micro Channel Provoked by Radiation and First Order Chemical Reaction. Asian Journal of Physical and Chemical Sciences 7(1) (2019), 1-14.
[40] B. D.Gupta, Mathematical Physics (Third Revised Edition). Viskas Publishing House PVT LTD, New Delhi (2005).
[41] M. D. Raisinghania, Advanced Differential Equations (Fourteenth Revised Edition). S.Chand and Company LTD. New Delhi (2011)